

# Hadronic final states and QCD studies at HERA\*

C. GLASMAN<sup>†</sup>

(ON BEHALF OF THE ZEUS AND H1 COLLABORATIONS)

Universidad Autónoma de Madrid

Results on QCD studies from the H1 and ZEUS Collaborations at the  $ep$  collider HERA are presented and their impact on LHC physics discussed.

PACS numbers: 13.87.-a,13.87.Ce

## 1. Introduction

HERA is the only electron(positron)-proton collider in the world. It has been running since 1992, with a major upgrade of the accelerator during 2001-2002. The multipurpose H1 and ZEUS detectors have been collecting data steadily during these years. Pre-upgrade integrated luminosities of  $\sim 100 \text{ pb}^{-1}$  per experiment have already allowed the most accurate determination of the proton structure up to date. Both collaborations have also made important contributions in making tests and precision measurements of QCD and the electroweak sector of the Standard Model, search for new particles and new interactions, study of jet production and jet substructure, study of the structure of the photon, heavy flavour production, and investigation of diffraction and the structure of the pomeron.

This report deals with the tests of QCD on hadronic final states, concentrating mainly on the results from jet production. Multijet QCD production will be the main background for searches of Higgs, supersymmetric particles and new physics in general. Also, the luminosity of the colliding particles (partons from the protons) at LHC will be governed by QCD and so precise determinations of the protons parton distribution functions (PDFs) and the strong coupling constant,  $\alpha_s$ , will be crucial for any cross section measurement. In this sense,  $ep$  collisions at HERA provide a suitable environment to do precision studies of QCD in hadronic-induced reactions (as opposed

---

\* Talk given at “Physics at LHC”, 3-8 July 2006, Cracow, Poland.

† Ramón y Cajal Fellow.

to  $e^+e^-$  annihilations at LEP) in a cleaner set-up than in  $p\bar{p}$  collisions at Tevatron.

The main sources of jets at HERA are neutral current (NC) deep inelastic scattering (DIS), with  $Q^2 \gg \Lambda_{\text{QCD}}^2$ , where  $Q^2$  is the square of the momentum transfer, and photoproduction (PHP), with  $Q^2 \approx 0$ . Up to leading order (LO) in  $\alpha_s$ , jet production in NC DIS proceeds via the quark-parton model ( $Vq \rightarrow q$ , where  $V = \gamma^*$  or  $Z^0$ ), boson-gluon fusion ( $Vg \rightarrow q\bar{q}$ ) and QCD-Compton ( $Vq \rightarrow qg$ ) processes. The jet production cross section is given in perturbative QCD (pQCD) by the convolution of the proton PDFs and the partonic cross section. Only two kinematic variables are needed to characterise these processes; they can be taken as  $Q^2$  and Bjorken  $x$ . The inelasticity variable  $y$ , which gives the energy transfer in the proton rest frame, is also useful. In PHP, a quasi-real photon emitted by the electron beam interacts with a parton from the proton to produce two jets in the final state. In LO QCD, there are two processes which contribute to the jet photoproduction cross section: the resolved process, in which the photon interacts through its partonic content, and the direct process, in which the photon interacts as a point-like particle. The jet production cross section is given by the convolution of the flux of photons in the electron, the parton densities in the proton and photon and the partonic cross section. Thus, measurements of jet cross sections in NC DIS and PHP can be used to perform tests of pQCD, help to constrain the gluon density in the proton and determine  $\alpha_s$ .

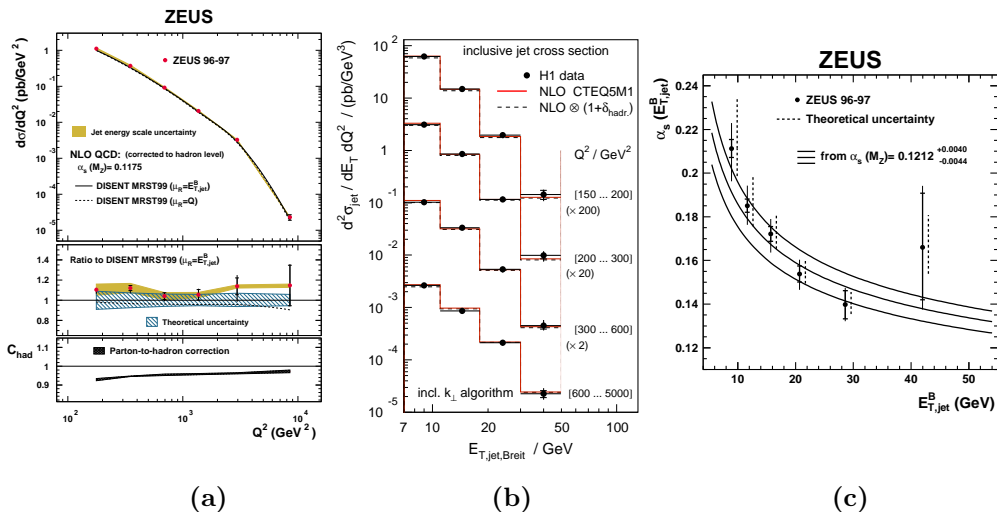


Fig. 1. (a) Inclusive-jet cross section in NC DIS as a function of  $Q^2$  [1]; (b) inclusive-jet cross section in NC DIS as a function of  $E_{T,B}^{\text{jet}}$  in different regions of  $Q^2$  [2]; (c) energy-scale dependence of  $\alpha_s$  [1].

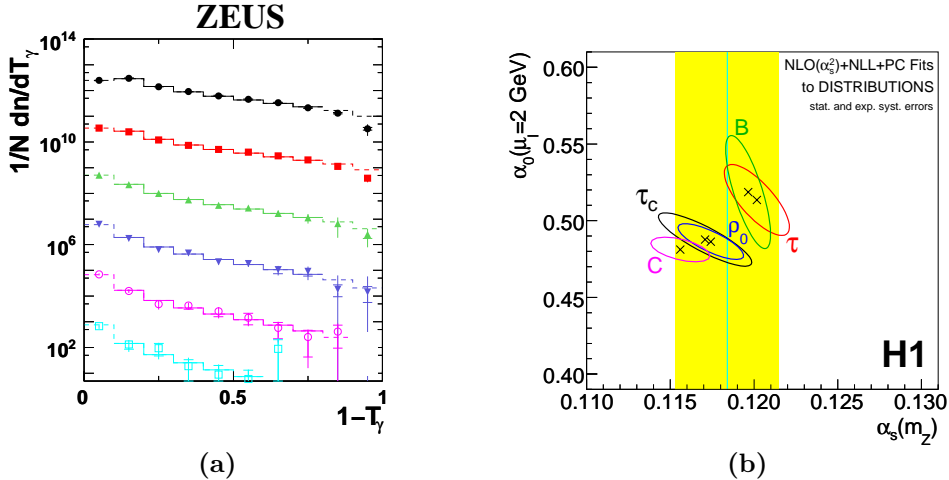


Fig. 2. (a) Thrust distribution in different  $Q^2$  regions [3]; (b)  $\bar{\alpha}_0$  and  $\alpha_s(M_Z)$  values extracted from event-shape distributions [4].

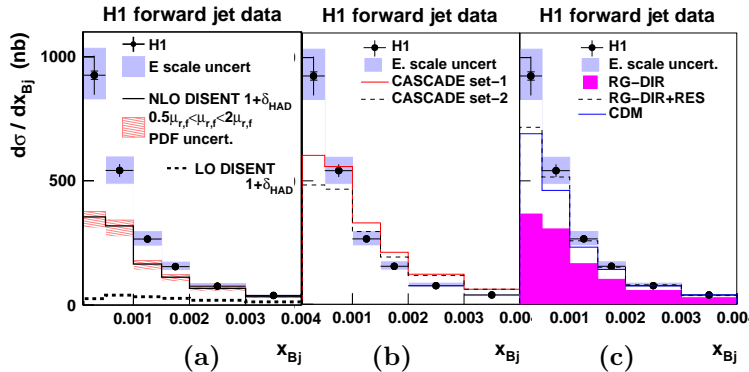


Fig. 3. Forward-jet cross section as a function of Borken  $x$  [5] compared to (a) LO and NLO calculations; (b) CASACADE MC predictions; and (c) CDM and RAPGAP MC predictions.

## 2. Jet search in $ep$ collisions

Jets in hadronic collisions are not as easily identified as in  $e^+e^-$  annihilations since the initial-state colliding partons carry only a fraction of the energy of the parent hadrons and are accompanied by several soft hadrons not correlated with the hard interaction. The spectator partons give rise to the so-called remnant jets (hadronisation of spectator partons), underlying event (soft interactions between the spectator partons) and multiparton interactions (hard interactions between the spectator partons).

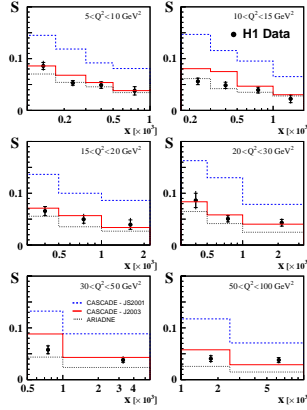


Fig. 4. Azimuthal correlation as a function of  $x$  for different  $Q^2$  regions [6] compared to the CDM and CASACADE MC predictions.

ZEUS

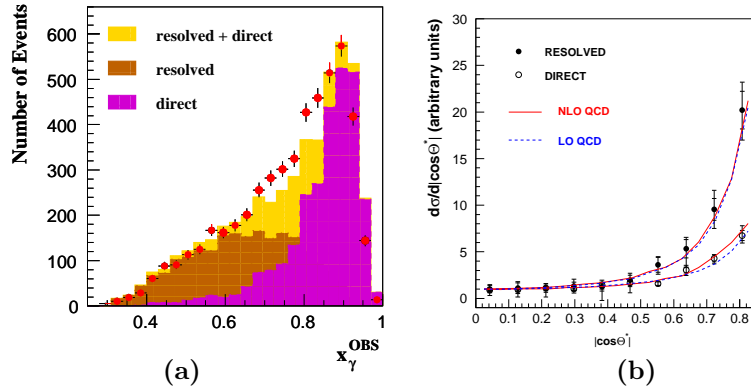


Fig. 5. (a)  $x_\gamma^{\text{obs}}$  distribution for data and resolved, direct and resolved+direct MC events [7]; (b) Dijet cross section as a function of  $|\cos \theta^*|$  in PHP for  $x_\gamma^{\text{obs}} \leq 0.75$  [7].

The collisions in hadronic-type reactions do not occur in the centre-of-mass frame; the initial-state partonic system is boosted along the beam axis by an amount which is different for every event. To treat on equal footing all possible final-state hadronic systems, variables invariant under longitudinal boosts, such as transverse energy ( $E_T$ ), differences in pseudorapidity ( $\eta$ ) and azimuth ( $\phi$ ), are best suited to reconstruct jets in this type of reactions. Also, the use of the transverse energy helps to identify the signal for a hard scattering and to disentangle the products of the hard interaction from the beam remnants. These features apply to both NC DIS and PHP processes at HERA, though in NC DIS there is a further complication due to the fact that the exchanged boson is virtual and carries  $p_T$ . This effect is compensated

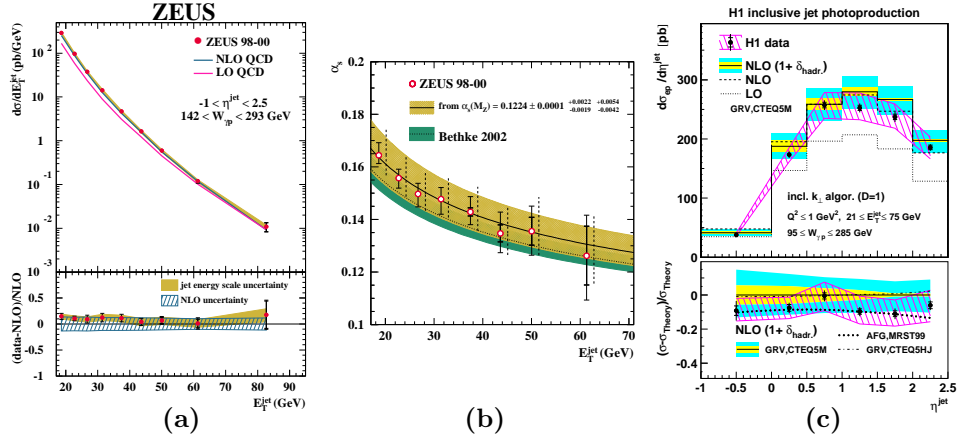


Fig. 6. (a) Inclusive-jet cross section as a function of  $E_T^{\text{jet}}$  [8]; (b)  $\alpha_s$  as a function of  $E_T^{\text{jet}}$  [8]; (c) inclusive-jet cross sections as a function of  $\eta^{\text{jet}}$  [9].

### ZEUS

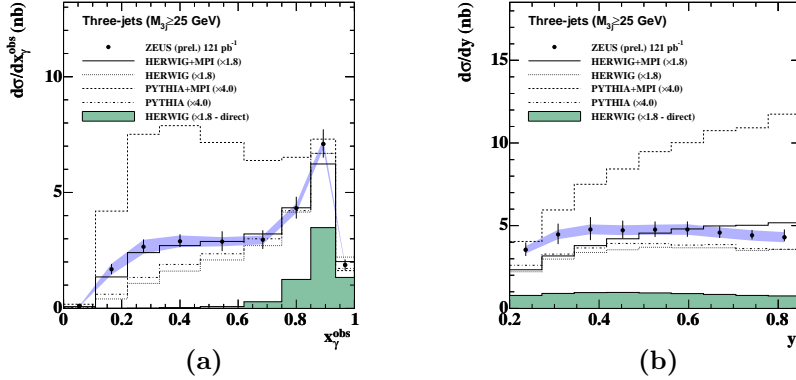


Fig. 7. Three-jet cross sections in PHP for  $M^{3j} > 25$  GeV as functions of (a)  $x_{\gamma}^{\text{obs}}$  and (b)  $y$  [14]. For comparison, the predictions of PYTHIA and HERWIG with and without MPIs are included.

for by selecting a frame in which the virtual boson and the proton collide head-on. This is the so-called Breit frame.

At HERA, the  $k_T$  cluster algorithm in the longitudinal inclusive mode has been proven to be the best algorithm to reconstruct jets in these hadronic-type reactions. This algorithm has been used by both the H1 and ZEUS collaborations since many years for making precision tests of pQCD. The advantages of this algorithm can be summarised as follows: (i) it allows a transparent translation of the experimental set-up to the theoretical calculations (it avoids the ambiguities related to overlapping and merging of jets present in cone algorithms); (ii) pQCD calculations using this algorithm are finite to all orders (as opposed to the cone algorithm, for which the

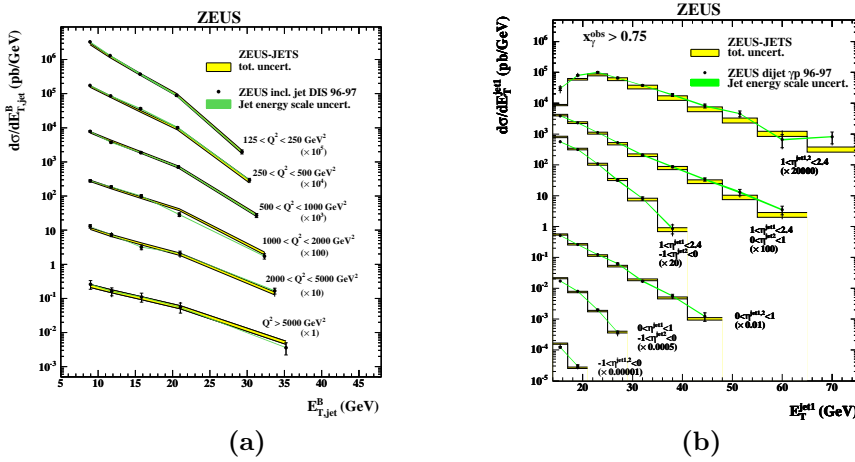


Fig. 8. (a) Inclusive-jet cross section in NC DIS as a function of  $E_{T,B}^{jet}$  in different regions of  $Q^2$  [1]; (b) Dijet cross section in PHP as a function of  $E_T^{jet}$  in different regions of  $\eta^{jet}$  for  $x_\gamma^{obs} > 0.75$  [7]. Both measurements are compared to NLO calculations based on ZEUS-jets proton PDFs [13].

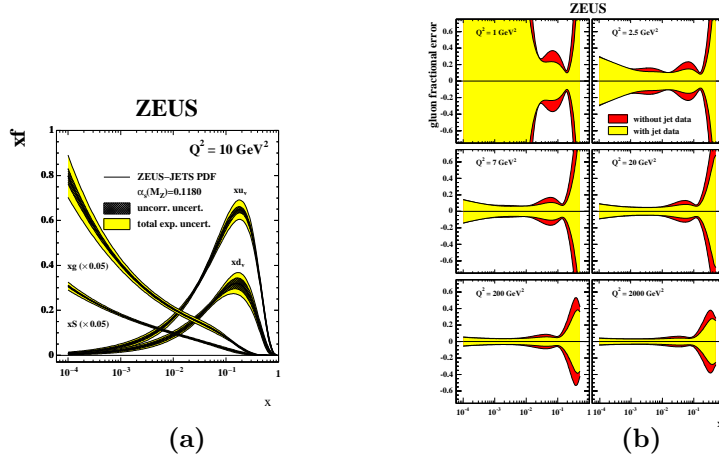


Fig. 9. (a) Valence, sea and gluon distributions from the ZEUS-jets proton PDF parametrisations [13]; (b) uncertainties of the ZEUS-jets proton PDF parametrisations [13].

calculations diverge for orders higher than the next-to-leading); and (iii) it presents the smallest hadronisation corrections compared to other algorithms. This algorithm has been used to reconstruct the jets in data and theoretical predictions for the measurements presented in the next sections.

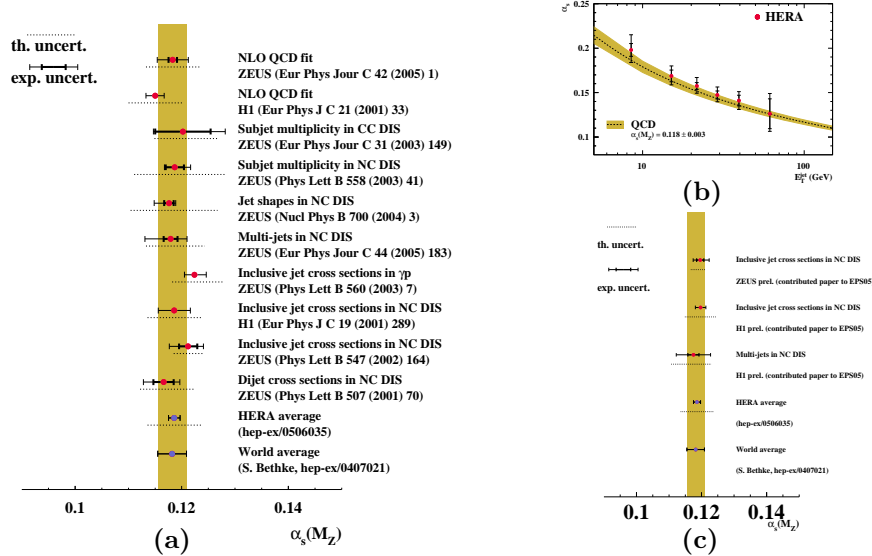


Fig. 10. (a,b) Summary of  $\alpha_s(M_Z)$  measurements at HERA compared with the world and HERA averages [11]; (b) combined measurements of  $\alpha_s(E_T^{\text{jet}})$  from HERA [11].

### 3. QCD studies in neutral current deep inelastic scattering

#### 3.1. Inclusive-jet cross sections and $\alpha_s$

Inclusive-jet cross sections have been measured in NC DIS at large  $Q^2$  ( $Q^2 > 125$  GeV $^2$  [1] and  $Q^2 > 150$  GeV $^2$  [2]) as functions of  $Q^2$ , the jet transverse energy in the Breit frame ( $E_{T,B}^{\text{jet}}$ ) and for  $E_{T,B}^{\text{jet}}$  in different regions of  $Q^2$  (see Fig. 1). The measured cross sections as functions of  $Q^2$  and  $E_{T,B}^{\text{jet}}$  display a steep fall-off of several orders of magnitude within the measured range; the data show a harder spectrum in  $E_{T,B}^{\text{jet}}$  as  $Q^2$  increases. The measurements have been compared to next-to-leading-order (NLO) QCD calculations. The predictions give a good description of the data over a wide range of  $Q^2$  and  $E_{T,B}^{\text{jet}}$ . This proves the validity of the description of the dynamics of inclusive-jet production by pQCD at  $\mathcal{O}(\alpha\alpha_s^2)$ . The LO prediction for the jet cross section in the Breit frame is directly proportional to  $\alpha_s$ . Values of  $\alpha_s(M_Z)$  have been extracted from the measurements:

$$\alpha_s(M_Z) = 0.1212 \pm 0.0017 \text{ (stat.)} \pm 0.0023 \text{ (exp.)} \pm 0.0028 \text{ (th.)} \quad (Q^2 > 500 \text{ GeV}^2),$$

$$\alpha_s(M_Z) = 0.1186 \pm 0.0030 \text{ (exp.)} \pm 0.0051 \text{ (th.)} \quad (Q^2 > 150 \text{ GeV}^2),$$

The small experimental (2.9% and 2.5%, respectively) and theoretical (2.3% and 4.3%, respectively) uncertainties make these determinations the most precise at HERA and comparable to those values extracted from more

inclusive measurements. The energy-scale dependence of  $\alpha_s$  has been tested from the measurements of the inclusive-jet cross section as a function of  $E_{T,B}^{\text{jet}}$ . The results, shown in Fig. 1(c), are in very good agreement with the running of  $\alpha_s$  as predicted by pQCD over a wide range in  $E_{T,B}^{\text{jet}}$ .

### 3.2. Event shapes and the hadronisation process

The hadronic final-state in NC DIS has also been used to study the hadronisation process, which is a non-perturbative effect. Recent developments in the model of power corrections permit the understanding of these effects from first principles. The model of Dokshitzer *et al.* is characterised by an effective universal coupling,  $\bar{\alpha}_0$ . Event-shape variables, like thrust, broadening,  $C$  parameter and jet mass (inspired by  $e^+e^-$  measurements), are well suited to test the universality of this effective coupling. In this type of analysis, the data are compared to a model prediction which consists of a combination of NLO QCD calculations and the expectations of the power-correction model:  $F = F_{\text{perturbative}} + F_{\text{power correction}}$ , where  $F$  is an event-shape mean or distribution. In the case of distributions, the perturbative prediction is supplemented by matched resummed calculations. Figure 2(a) shows, as an example, the measured thrust distribution in different regions of  $Q^2$  [3] together with the predictions which have been fitted to the data to extract  $\bar{\alpha}_0$  and  $\alpha_s(M_Z)$ . It is possible to obtain a good description of the event-shape observables in hadronic-induced reactions in the regions of phase space where the predictions of the power-correction model are valid. The results of the fits to extract  $\bar{\alpha}_0$  and  $\alpha_s(M_Z)$  are shown, for all event-shape observables measured, in Fig. 2(b) [4]. The extracted  $\alpha_s(M_Z)$  values are consistent for all observables and with the world average (shaded band). It is possible to extract a universal non-perturbative parameter,  $\bar{\alpha}_0 = 0.5 \pm 10\%$ , from all the measured observables. This supports the concept of power corrections as an appropriate alternative approach for the description of hadronisation effects.

### 3.3. Parton evolution at low $x$ and unintegrated PDFs

One of the main channels of Higgs production at LHC is expected to be  $gg \rightarrow H$ . Predictions for this process need information on the parton evolution at low  $x$  and on the unintegrated proton PDFs. Forward-jet data at HERA are ideally suited to study these effects.

At high scales ( $Q, E_T^{\text{jet}}$ ), NLO calculations using the DGLAP evolution equations provide a good description of the data (see Section 3). Thus, measurements at HERA have provided accurate determinations of the proton PDFs and precise determinations of  $\alpha_s$ . The DGLAP evolution is equiva-

lent to the exchange of a parton cascade in which the exchanged partons are strongly ordered in virtuality  $k_T$ . This approximation works well at high scales, as mentioned above, but it is expected to break down at low  $x$  since it includes only resummation of leading logarithms in  $Q^2$  and neglects contributions from  $\log 1/x$ , which are important when  $\log Q^2 \ll \log 1/x$ . Approaches to parton evolution which deal with low  $x$  comprise: (i) BFKL evolution, which includes resummation of  $\log 1/x$  terms and exhibits no  $k_T$  ordering; (ii) the CCFM equations, which incorporate angular-ordered parton emission and are equivalent to BFKL for  $x \rightarrow 0$  and to DGLAP at large  $x$ ; (iii) the introduction of a second  $k_T$ -ordered parton cascade on the photon side à la DGLAP, which is implemented by assigning a partonic structure to the virtual photon, mimicks higher-order QCD effects at low  $x$ . HERA is an ideal testbed for these theoretical approaches. These tests are realised by restricting the jet data to large jet pseudorapidity values (forward direction, proton side),  $x_{\text{jet}} \equiv E_T^{\text{jet}}/E_p \gg x_{\text{Bj}}$  (to suppress quark-parton-model type events) and  $Q \approx E_T^{\text{jet}}$  (to restrict evolution in  $Q^2$ ).

Figure 3 shows the measured forward-jet data [5] as a function of Bjorken  $x$ . The data increases as  $x_{\text{Bj}}$  decreases. The data are compared to different predictions. The NLO pQCD calculations, based on DGLAP evolution equations, fail to describe the data at low  $x$ . The predictions of the CASCADE Monte Carlo (MC), which is an implementation of the CCFM equations, give an improved description of the data at low  $x$ , but the description at high  $x$  worsens. The predictions of the CDM model, which contain no- $k_T$  ordering, and the resolved-photon MC give a better description of the data, except at very low  $x$ .

Insight into low- $x$  dynamics can also be gained by studying the azimuthal separation ( $\Delta\phi$ ) between the two hardest jets. An excess of events at small  $\Delta\phi$  would signal a deviation from DGLAP evolution. The fraction  $S$  of dijet events with  $\Delta\phi < 120^\circ$  has been measured [6] as a function of Bjorken  $x$  in different regions of  $Q^2$ . The data are shown in Fig. 4 compared with different predictions. The predictions of the CDM model give a good description of the data at low  $x$  and low  $Q^2$ , but are below the data for high  $Q^2$ . The predictions of the CASCADE MC using different sets of unintegrated PDFs are also shown: the predictions display sensitivity to the unintegrated gluon distributions. Therefore, these measurements can be used to constrain the unintegrated PDFs.

## 4. QCD studies in photoproduction

### 4.1. Test of color dynamics in dijet PHP

Measurements of jet cross sections in PHP allow tests of color dynamics. At HERA, quark and gluon exchange can be studied in dijet PHP by

separating resolved and direct processes using the fraction of the photon energy invested in the production of the dijet system, which is measured via the observable  $x_\gamma^{\text{obs}} = \sum E_T^{\text{jet}_i} e^{-\eta^{\text{jet}_i}} / 2yE_e$ . For direct events,  $x_\gamma^{\text{obs}} \sim 1$  and for resolved events,  $x_\gamma^{\text{obs}} < 1$ . Resolved processes are dominated by gluon exchange (like dijets in  $pp$  collisions) and the angular behaviour of the cross sections is  $\propto (1 - |\cos \theta^*|)^{-2}$  for  $\theta^* \rightarrow 0$  (Rutherford scattering), where  $\theta^*$  is the scattering angle in the dijet centre-of-mass frame. Direct processes proceed via quark exchange (similar to prompt-photon processes in  $pp$  collisions) and the angular behaviour of the cross section is  $\propto (1 - |\cos \theta^*|)^{-1}$  for  $\theta^* \rightarrow 0$ . Therefore, the  $\cos \theta^*$  distribution reflects the underlying parton dynamics since it has sensitivity to the spin of the exchanged particle in two-body processes.

The data sample for  $x_\gamma^{\text{obs}} > (<)0.75$  is expected to be dominated by direct (resolved) processes, as demonstrated by the  $x_\gamma^{\text{obs}}$  distribution for data and resolved, direct and resolved+direct MC events shown in Fig. 5(a) [7]. These samples were used to compute the cross section as a function of  $|\cos \theta^*|$  (see Fig. 5(b)) [7]. The cross sections increase as  $|\cos \theta^*|$  increases, but the cross section for  $x_\gamma^{\text{obs}} < 0.75$  displays a much more rapid increase for  $|\cos \theta^*| \rightarrow 1$  than the cross section for  $x_\gamma^{\text{obs}} > 0.75$ . The LO and NLO QCD calculations, which include resolved (direct) processes with an angular behaviour  $\propto (1 - |\cos \theta^*|)^{-2(-1)}$  give a very good description of the data. This demonstrates that the underlying parton dynamics in PHP is well understood.

#### 4.2. Inclusive-jet cross sections, $\alpha_s$ and the photon PDFs

Measurements of jet cross sections in PHP allow tests of pQCD. Inclusive-jet cross sections have been measured in PHP at large  $E_T^{\text{jet}}$  ( $E_T^{\text{jet}} > 17$  GeV [8] and  $E_T^{\text{jet}} > 21$  GeV [9]) as functions of  $E_T^{\text{jet}}$  and  $\eta^{\text{jet}}$  (see Figs. 6(a) and (c), respectively). The measured cross section as a function of  $E_T^{\text{jet}}$  displays a steep fall-off of several orders of magnitude within the measured range. The measurements have been compared to NLO QCD calculations. The predictions give a good description of the data. This proves the validity of the description of the dynamics of inclusive-jet production by pQCD at  $\mathcal{O}(\alpha\alpha_s^2)$ . The QCD prediction for the jet cross section is directly proportional to  $\alpha_s$ . A value of  $\alpha_s(M_Z)$  has been extracted from the measurement of  $d\sigma/dE_T^{\text{jet}}$ :

$$\alpha_s(M_Z) = 0.1224 \pm 0.0001 \text{ (stat.)} \quad {}^{+0.0022}_{-0.0019} \text{ (exp.)} \quad {}^{+0.0054}_{-0.0042} \text{ (th.)}.$$

The small experimental (1.8%) and theoretical (4.4%) uncertainties make this determination also one of the most precise at HERA. This value and the ones quoted in Section 3.1 are in agreement with the world [10] and HERA [11] averages. The energy-scale dependence of  $\alpha_s$  has been tested

from the measurements of the inclusive-jet cross section as a function of  $E_T^{\text{jet}}$ . The results, shown in Fig. 6(b), are in very good agreement with the running of  $\alpha_s$  as predicted by pQCD over a wide range in  $E_T^{\text{jet}}$ .

Measurements of jet cross sections in PHP also allow tests of the photon PDFs. The structure of the photon can be investigated at HERA by measuring jet cross sections most sensitive to the photon PDFs, namely  $d\sigma/d\eta^{\text{jet}}$  (see Fig. 6(c)) [9] or  $d\sigma/dx_\gamma^{\text{obs}}$ , and comparing the measurements to predictions based on different parametrisations of the PDFs. The measurements can then be used to discriminate among different parametrisations or used in a global fit to constrain them, as it was recently done for the proton PDFs (see Section 5).

#### 4.3. Multijet cross sections and multiparton interactions

Measurements of jet cross sections in PHP allow tests of hard multijet production and multiparton interactions (MPIs), which are expected to be copious at LHC energies. Multijet production is directly sensitive to higher orders since e.g. the three-jet cross section is proportional to  $\alpha_s^2$  at lowest order. Such measurements allow tests of the parton showers in the MC models. Their sensitivity to MPIs allows tests and tuning of the models. Figure 7 shows the three-jet cross section for  $M^{3j} > 25$  GeV as functions of  $x_\gamma^{\text{obs}}$  and  $y$  [14]. The data are compared to the predictions of the PYTHIA and HERWIG MC models which describe the shape of the  $y$  distribution but fail to describe the shape of the measured  $x_\gamma^{\text{obs}}$  distribution. The inclusion of MPIs in PYTHIA, tuned to generic collider data, results in a failure to describe both data distributions. In the case of HERWIG, the MPI model was tuned to the  $x_\gamma^{\text{obs}}$  distribution and gives a good description of the data, but the description of  $y$  gets spoiled. Therefore, these very precise data are an ideal ground for tuning and testing the parton-shower and MPI models in a clean hadronic-induced environment.

### 5. Jet cross sections and the proton PDFs

Measurements of jet cross sections in NC DIS and PHP are directly sensitive to the proton PDFs and provide a useful constrain on the gluon density, especially at mid- to high- $x$  values, which are most relevant at LHC energies. This is achieved in the case of PHP by restricting the measurements to regions of phase space less sensitive to the photon PDFs, i.e.  $x_\gamma^{\text{obs}} > 0.75$ . Recently, very precise measurements of inclusive-jet cross sections in NC DIS as a function of  $E_{T,B}^{\text{jet}}$  in different regions of  $Q^2$  (see Fig. 8(a)) [1] and dijet cross sections in PHP as a function of  $E_T^{\text{jet}}$  in different  $\eta^{\text{jet}}$  regions for  $x_\gamma^{\text{obs}} > 0.75$  (see Fig. 8(b)) [12] have been incorporated in a rigorous way in

a QCD fit to determine the proton PDFs [13]. The valence, sea and gluon distributions as a function of  $x$  for  $Q^2 = 10$  GeV $^2$  are shown in Fig. 9(a). The incorporation of jet cross sections in the fit resulted in an improvement on the determination of the gluon density in the proton: as shown in Fig. 9(b), the uncertainty in the gluon density decreases for mid- to high- $x$  by up to a factor of two.

## 6. Conclusions

HERA has become an unique QCD-testing machine, very useful for understanding multijet production in clean hadronic-induced reactions. Considerable progress in understanding and reducing uncertainties has led to very precise determinations of  $\alpha_s$  (see Fig. 10(a)). The dominant uncertainty in these measurements comes from the theoretical side thus, improved QCD calculations are needed for better accuracy. The running of  $\alpha_s$  has been observed from HERA jet data alone (see Fig. 10(b)). New HERA I results are still coming; new determinations of  $\alpha_s(M_Z)$  are shown in Fig. 10(c) and more than 400 pb $^{-1}$  of integrated luminosity of  $e^\pm p$  data with polarised lepton beams are being analysed. Therefore, there is a wealth of hadronic-type-reaction data already available to test new MC models, MC@NLO and next-to-next-to-leading-order pQCD calculations if they are made available for  $ep$  collisions.

## REFERENCES

- [1] ZEUS Coll., S. Chekanov *et al.*, *Phys. Lett.* **B** 547 (2002) 164.
- [2] H1 Coll., C. Adloff *et al.*, *Eur. Phys. Jour.* **C** 19 (2001) 289.
- [3] ZEUS Coll., S. Chekanov *et al.*, DESY 06-042.
- [4] H1 Coll., A. Aktas *et al.*, *Eur. Phys. Jour.* **C** 46 (2006) 343.
- [5] H1 Coll., A. Aktas *et al.*, *Eur. Phys. Jour.* **C** 46 (2006) 27.
- [6] H1 Coll., A. Aktas *et al.*, *Eur. Phys. Jour.* **C** 33 (2004) 477.
- [7] ZEUS Coll., M. Derrick *et al.*, *Phys. Lett.* **B** 384 (1996) 401.
- [8] ZEUS Coll., S. Chekanov *et al.*, *Phys. Lett.* **B** 560 (2003) 7.
- [9] H1 Coll., C. Adloff *et al.*, *Eur. Phys. Jour.* **C** 29 (2003) 497.
- [10] S. Bethke, hep-ex/0407021.
- [11] C. Glasman, hep-ex/0506035.
- [12] ZEUS Coll., S. Chekanov *et al.*, *Eur. Phys. Jour.* **C** 23 (2002) 4.
- [13] ZEUS Coll., S. Chekanov *et al.*, *Eur. Phys. Jour.* **C** 42 (2005) 1.
- [14] ZEUS Coll., S. Chekanov *et al.*, ZEUS-prel-06-009.